PERFORMANCE OF INELASTIC, SHALLOW FOUNDED STRUCTURES ON LIQUEFIABLE GROUND AND THE EFFECTIVENESS OF MITIGATION STRATEGIES

B. Paramasivam[1], S. Dashti[2], A.B. Liel[3], J.C. Olarte[4], L.D. Souza Junior[5], L. Soligo Gomes[6]

[1] *Graduate student, University of Colorado, Boulder, U.S.A., Balaji.Paramasivam@colorado.edu*
[2] *Assistant Professor, University of Colorado, Boulder, U.S.A., Shideh.Dashti@colorado.edu*
[3] *Associate Professor, University of Colorado, Boulder, U.S.A., Abbie.Liel@colorado.edu*
[4] *Graduate student, University of Colorado, Boulder, U.S.A., Juan.Olarte@colorado.edu*
[5] *Undergraduate student, University of Colorado, Boulder, U.S.A., Luciano.Souzajunior@colorado.edu*
[6] *Undergraduate student, University of Colorado, Boulder, U.S.A., Leonardo.SoligoGomes@colorado.edu*

Abstract

The risk of damage to the built environment from liquefaction can be significant. Soil settlements and differential displacements coupled with ground shaking can cause significant damage to structures and lifelines. Yet, the influence of soil liquefaction and different remediation strategies on the performance and damage potential of structures is not well understood, hindering the development of an effective, performance-based mitigation methodology. This paper presents the results of a centrifuge experiment conducted at the University of Colorado Boulder, in which a 3-story building with potential for inelastic behavior was founded on a layered soil deposit, including a liquefiable layer. The influence of two mitigation techniques, enhanced drainage and in-ground structural confinement, on the performance of the building during earthquake loading was investigated. The test results showed that remediation with stiff structural walls can reduce permanent foundation settlement and rotation during less intense motion, but can amplify settlements during more intense shaking that cause liquefaction under the footing. In all cases, the structural wall amplifies transient foundation rotation. Enhanced drainage with vertical pre-fabricated drains reduces excess pore pressure generation under the structure as well as foundation settlement and rotation, but it increases the flexural drift and floor accelerations.

Keywords: Centrifuge; Liquefaction; Inelastic Structures; Soil-Structure Interaction; Mitigation; Settlement;

1. Introduction

Previous earthquakes (e.g., the 1964 Alaska, 1990 Luzon, 1999 Dagupan, 1999 Kocaeli, and 2011 Christchurch earthquakes) have repeatedly demonstrated the damaging effects of soil liquefaction on buildings. In particular, buildings located on liquefiable soil deposits underwent permanent differential settlement, lateral spreading and tilt, punching, and bearing capacity failure, resulting in significant economic losses. Mitigating the liquefiable soil has the potential to the reduce soil's tendency for excess pore pressure generation and large permanent settlements. However, mitigation may at times amplify tilt, or may increase demands on the structural elements. The consequences of mitigation in terms of building performance are not well understood, due to lack of detailed field case histories and physical model studies.

In this study, a centrifuge test was conducted to examine the effects of two liquefaction remediation techniques on the performance of a three-story inelastic structure: 1) enhanced drainage; and 2) ground reinforcement via a structural wall. Seismic soil-mitigation-structure interaction is explored first by comparing the soil response underneath the structure with the far-field. Then, the influence of two mitigation techniques on building response is explored in terms of foundation settlement, tilt, story drift, and the structure's moment-rotation behavior. The experimental observations presented in this paper aim to provide insights into the effectiveness of two types of remediation strategies in the context of building performance.

2. Background

Liquefaction-induced ground settlement and lateral spreading can damage building structures. Several researchers have used case histories and physical model studies to evaluate the seismic performance of shallow-founded structures on liquefiable soil deposits [1-4]. They typically observed that significant building settlement happens during shaking, with less contribution from post-shaking reconsolidation settlements. Also, foundation settlement was often greater than that in the far-field. Dashti et al. [3-4] performed four centrifuge experiments to identify the dominant mechanisms of earthquake-induced building settlement on relatively thin liquefiable soil deposits. The primary mechanisms concluded in this study were: 1) volumetric types: rapid drainage ($\varepsilon_{p\text{-}DR}$), sedimentation ($\varepsilon_{p\text{-}SED}$), and consolidation ($\varepsilon_{p\text{-}CON}$); and 2) deviatoric types: partial bearing capacity loss ($\varepsilon_{q\text{-}BC}$) and soil-structure interaction (SSI) induced building ratcheting ($\varepsilon_{q\text{-}SSI}$). Despite significant strides toward a better understanding of the liquefaction phenomenon and its consequences, the current state of practice for evaluating building performance and the effectiveness of mitigation techniques still primarily relies on empirical procedures that estimate settlement assuming free-field conditions [5-6]. These procedures are known to largely underestimate building settlements.

When liquefaction triggering is a concern in the design phase, the hazard can be mitigated, in order to either reduce the likelihood of large excess pore pressure generation or to limit the resulting displacements. Stewart et al. [7] provided a comprehensive review of field and 1g shake table studies of different liquefaction mitigation techniques such as densification, drainage, and in-ground walls.

Liu and Dobry [1] performed centrifuge tests of liquefiable soil models with and without densifying the soil under a model rigid shallow footing. They showed that foundation settlement on a densified soil was significantly reduced. Later, physical model studies of soil densification in a bridge site by Balakrishnan and Kutter [8] showed that densification increases the stiffness and shear resistance of the soil deposit, but alters the predominant period of the site, leading to an increase or decrease in the amplitude of the ground motion associated with changes in frequency content, which may be damaging to the superstructure.

An alternative to soil densification is enhanced drainage in the liquefiable soil using gravel drains, stone columns, or vertical composite drains [9-12]. Sasaki and Taniguchi [9] conducted a series of 1g shaking table tests on a large tank (length = 12m, width = 2m, and depth = 3m), which contained a uniform loose sandy soil deposit with the model structure embedded to a depth of 1m from the surface. The test was undertaken with and without gravel drains. The results suggested that the gravel drains reduced the magnitude of excess pore pressures underneath the structure. Moreover, the presence of the gravel drains modified the flow patterns inside the soil, thereby accelerating the rate of pore pressure dissipation in the liquefiable layer. Vertical composite

drains are a more recent invention for providing drainage in the liquefiable soil deposit with minimum reinforcement [11-12]. Their performance has not been evaluated extensively in the field or centrifuge, particularly near structures.

In-ground structural walls provide another alternative approach for isolating the building from a liquefiable soil mass [3,4,10,13]. Tanaka et al. [13] evaluated the performance of sheet piles as liquefaction mitigation for a tunnel structure in a 1g shake table test indicating that ground settlement reduced by 75% for the case of soil with sheet-pile walls. Centrifuge model tests conducted by Dashti et al. [4] showed that installation of a stiff structural wall can minimize seismic-induced deviatoric strains and localized volumetric strain due to drainage, and hence reduce building settlements. Tanaka et al. [13] further showed that sheet-pile walls with draining elements provide strength, but also reduce the excess pore pressures in the soil compared to soil mitigated only with sheet piles.

Physical model studies reported in the literature have in the past primarily focused on single-degree-of-freedom (SDOF), linear-elastic buildings [3-4] or footing-only models [1] that captured the bearing pressure alone. A small number of centrifuge studies have been conducted to study the performance of inelastic structures on dry sand [14-15]. However, there is need for additional physical model studies to better understand the behavior of inelastic structures (i.e., capable of damage) on liquefiable soil deposits, in order to properly evaluate the effectiveness of liquefaction remediation strategies in the context of building performance and damage potential.

3. Centrifuge experimental setup

A dynamic centrifuge test was performed using the 5.5m radius centrifuge facility at the University of Colorado Boulder [16]. A layered soil specimen, including a liquefiable layer, with two model structures (Fig. **1**), was spun at a centrifugal acceleration of 70g. The model was subject to a series of 1-D horizontal earthquake motions in flight using the servo-hydraulic shake table in centrifuge [17]. Fig. 1 shows the cross sectional view of the model and the instruments (accelerometers, pore pressure transducers, and LVDTs) installed during model preparation. Unless indicated otherwise, units provided in this paper are in prototype scale.

The liquefiable soil model was constructed in a new flexible shear beam (FSB) container of length 968mm, width of 376mm, and depth of 304mm. The FSB container consists of four hollow square aluminum rings stacked one above the other with thick rubber layers in between the rings. The rubber layer within the aluminum rings provides flexibility to the container and deforms along with the soil. The aluminum FSB container was fabricated using the procedure explained in Ghayoomi et al. [18]. The centrifuge soil model was prepared with relatively uniform, clean, and fine Ottawa sand (F-65). The properties of Ottawa sand were measured as: maximum void ratio (e_{max}) = 0.81, minimum void ratio (e_{min}) = 0.53, uniformity coefficient (c_u) = 1.56, and specific gravity of solids (G_s) = 2.65. The bottom dense layer of Ottawa sand with a thickness (*H*) of 18m was dry pluviated to achieve a relative density (D_r) of approximately 90%. This dense layer was overlaid by a looser liquefiable layer of Ottawa sand with $D_r \approx 40\%$ and H = 4m. Finally, a layer of Monterey sand (e_{max} = 0.84 and e_{min} = 0.54) with $D_r \approx 90\%$ and H = 2m was dry pluviated as the non-liquefiable surface layer.

The model structure used in this study was a 3-story potentially inelastic frame structure founded on a stiff mat foundation. Beams, columns, masses and fuses (areas of beam or column with a reduced cross-section) of the structure were made of steel and the mat foundation was fabricated using an aluminum plate. This model represented a prototype structure of width (*W*) 9.5m and height (*H*) 12.65m designed to represent a so-called "special" steel moment resisting frame in California. The contact pressure at the foundation level was estimated at 80 kPa and the fixed-base modal periods of the structure were measured to be 0.6, 0.15, and 0.06 s.

Fig. 1 shows two different liquefaction mitigation strategies employed around the two identical structures tested simultaneously: 1) enhanced drainage (identified as Structure-DR); and 2) in-ground structural walls (identified as Structure-SW). The soil surrounding Structure-DR was treated with model prefabricated vertical drains (PVDs). The model drains consisted of pipes to collect and transport pore water and geotextile filters around the pipes to prevent clogging. Model drain pipes were constructed using santoprene rubber of durometer 64A with an inner diameter of 3.17mm (model scale) and a length of 178.6mm. Holes were drilled through the

tube manually, which were 0.71mm (model scale) in diameter with a center-to-center spacing of 5mm along the length of the tube. Each model drain had a total of 216 holes with an area ratio of 2.09%, defined as the ratio of orifice area to the tube surface area. This santoprene rubber tube was wrapped with woven polyester filters with an aperture opening size of 0.178mm. This polyester mesh was used to avoid clogging with sand particles. The drains were inserted into the middle of the lower dense Ottawa sand layer, as shown in Fig. **1**. In total, 72 drains were installed in a triangular pattern around the perimeter of the foundation with a center-to-center distance of 17mm in model scale (1.2m in prototype scale). The liquefiable soil underneath Structure-SW was mitigated by constructing an in-ground structural wall around the perimeter of the foundation. This structural wall had a width of 152.4mm (model scale) and height of 178.6mm, and was placed inside the soil deposit to the mid-depth of dense Ottawa sand layer. The prototype flexural rigidity of the structural wall used in this study is 787.3 MN-m^2/m.
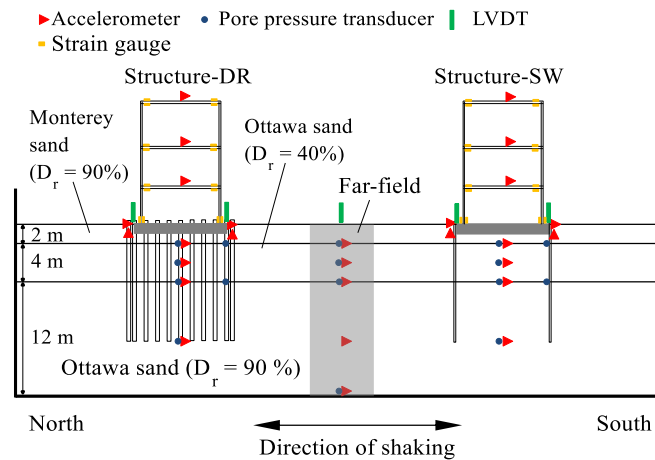

Fig. 1 – Instrumentation layout of centrifuge experiment showing the structures on soil mitigated with vertical pre-fabricated drains and in-ground structural walls.

In this study, a solution of hydroxypropyl methylcellullose was used as a pore fluid with a kinematic viscosity of approximately 64 cSt [19] to create a fluid 70 times more viscous than water and satisfy the scaling laws. During the saturation phase, the soil model with structures was initially flushed with CO_2 from the bottom of the container. Then, the model was kept under vacuum and the viscous pore fluid was slowly injected from the bottom of the container at a controlled rate. The rate of pore fluid flow was controlled constantly by the vacuum pressure difference between model and the fluid container, similar to the procedure proposed by [20].

A series of seven earthquake motions was applied at the base of the model, with sufficient time after each event to allow for the full dissipation of excess pore pressures. In this paper, results from two ground motions (Kobe and JoshuaT) are discussed in detail. Table **1**shows the properties of these two base motions as measured in the test.

Table 1 – Ground motion properties as recorded at the base of the container in centrifuge.

Ground Motion ID	Event	Station	PGA (g)	Sign. Duration, D_{5-95} (s)	Mean Period, T_m (s)	Arias Intensity, I_a (m/s)
Kobe	1995 Kobe	Takatori	0.37	14	0.83	1.7
JoshuaT	1992 Landers	Joshua Tree	0.39	28	0.68	5.1

4. PRELIMINARY RESULTS AND OBSERVATIONS

4.1 Soil response in the far-field and under the structures

Time histories of horizontal acceleration and excess pore pressure recorded in the far-field soil, located between Structure-DR and Structure-SW, are shown in Fig. 2 for the JoshuaT motion. The acceleration time history records in the liquefiable soil layer in the far-field show large acceleration spikes. These spikes are likely due to soil dilation and re-stiffening [3-4, 21]. During the JoshuaT event, an excess pore pressure ratio ($R_u = \Delta u / \sigma_v'$) of 1.0, indicating liquefaction, was reached in the far-field soon after shaking.
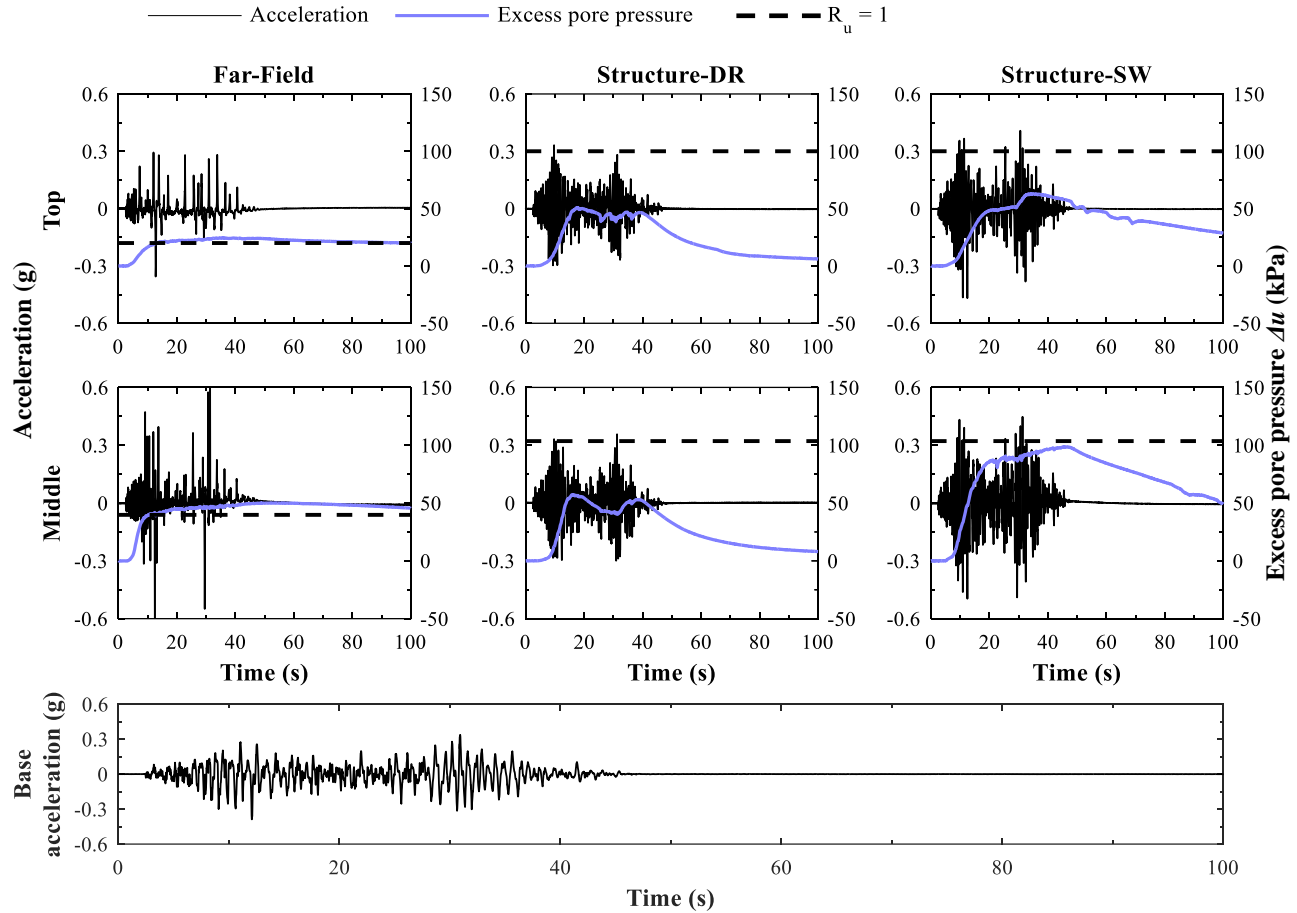
Fig. 2 – Acceleration and excess pore pressure time histories measured at top and middle of liquefiable layer during the JoshuaT motion.

Buildings, which include the foundation and the superstructure, impose confining stresses onto the underlying soil, providing resistance to liquefaction but also making the soil response less dilative. Results of excess pore pressures in soil underneath Structure-DR and Structure-SW shows that achieving an R_u of 1.0 is more difficult under the higher confining stress of the building compared to the far-field during the motions considered. This is generally the case both under the center and edge of the foundation. Indeed, the peak R_u measured under the center of Structure-DR is less than 0.6 during both motions. The model drains around the perimeter of the foundation effectively drain the excess pore pressure generated under the building and the water flowing toward the building from the far-field soil. Structure-SW, which is isolated by in-ground structural wall, shows a peak R_u of 0.97 at the middle of the liquefiable soil layer during the longer-duration JoshuaT motion. The structural wall acts as a water barrier to avoid water flow toward or from the surrounding soil. The large maximum R_u in soil measured at the center of Structure-SW is caused by 1D vertical flow of water from the dense sand layer to the surface. The flow in this case is slowed down by the boundaries of the structural wall.

4.2 Foundation settlement and rotation

Foundation settlement and rotation caused by seismic loading are measured using four vertical LVDTs placed at the corners of each building's footing. The average of the four LVDT recordings provides the average foundation settlement. The difference in LVDT recordings on the north and south ends of the footing (Fig. **1**), divided by the foundation width, provides a measure of foundation rotation (also referred to as tilt). The foundation settlement time histories on Structures-DR and SW during the Kobe and JoshuaT motions are compared in Fig. 3. The far-field settlements and the corresponding base accelerations are also plotted on the same figures for comparison. This figure shows that significant settlement occurs during shaking at all locations throughout the model, and the footing settlement is generally higher than that in the far-field, particularly during the stronger, longer-duration event (JoshuaT). Similar results have been reported by [1-4]. Settlements in the far-field are controlled by volumetric strains (reconsolidation and sedimentation), whereas deviatoric strains are also present under the structures.
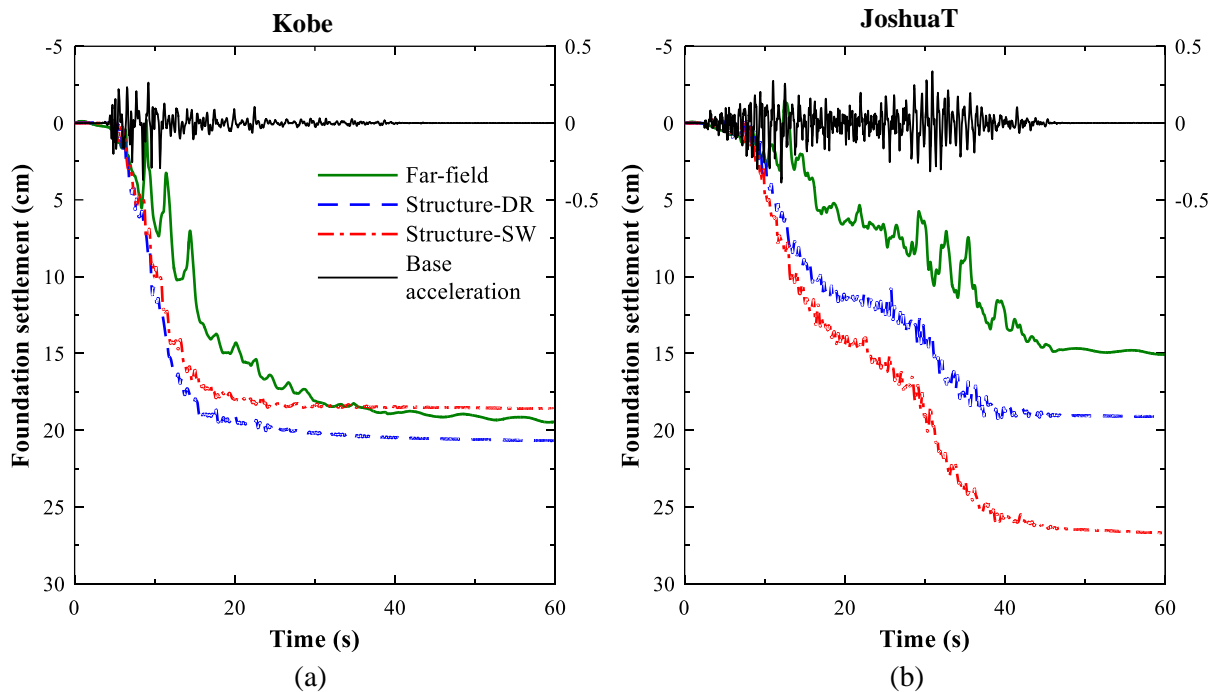

Fig. 3 – Time histories of foundation settlement compared to the far-field and base acceleration during the: (a) Kobe and (b) JoshuaT motions.

The test results also facilitate investigation of the role of mitigation techniques in foundation settlements. The stiff in-ground structural wall provides confinement to the soil deposit underneath the structure, restricting deviatoric type deformations (ε_{q-BC} and ε_{q-SSI}) and volumetric deformations due to flow during earthquake loading (ε_{p-DR}). The prefabricated vertical drains, on the other hand, successfully limit excess pore pressure generation underneath the building, which help reduce volumetric strains due to reconsolidation (ε_{p-CON}) as well as deviatoric strains caused by strength loss in the foundation soil and soil-structure interaction induced ratcheting (ε_{q-BC} and ε_{q-SSI}). During the less intense event, Structure-SW performs better in terms of settlement (about 11% less than Structure-DR), as shown in Fig. 3(a) . During the stronger motion (JoshuaT), however, Structure-SW experiences a settlement 41% greater than that of Structure-DR, as shown in Fig. 3(b). This is due to the triggering of soil liquefaction under Structure-SW (by inhibiting flow), which greatly amplifies volumetric type strains due to sedimentation (ε_{p-SED}), a mechanism that did not exist previously underneath the structures.

In addition to building settlement, tilt, which is induced by foundation rotation, is also of primary interest and concern, due to its significance for building performance and damage potential. Fig. 4(a) and (b) summarize the results of foundation rotation measured on Structure-DR and Structure-SW during the Kobe and JoshuaT

motions. The Fourier amplitude spectra (FAS) of foundation rotation during the Kobe and JoshuaT motions are also shown in Fig. 4.
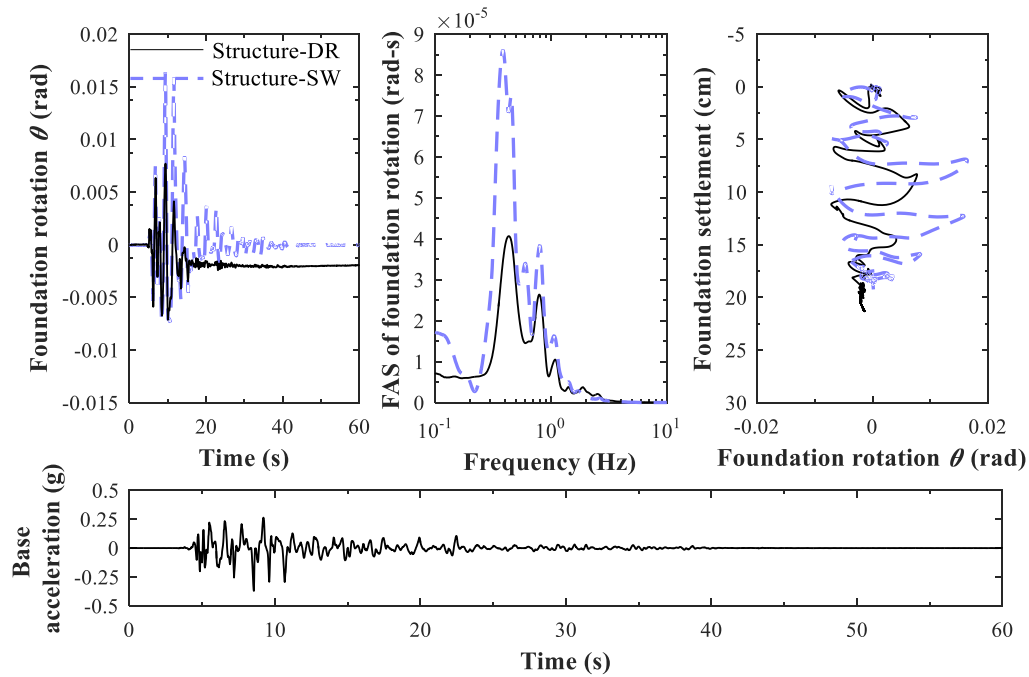
(a)
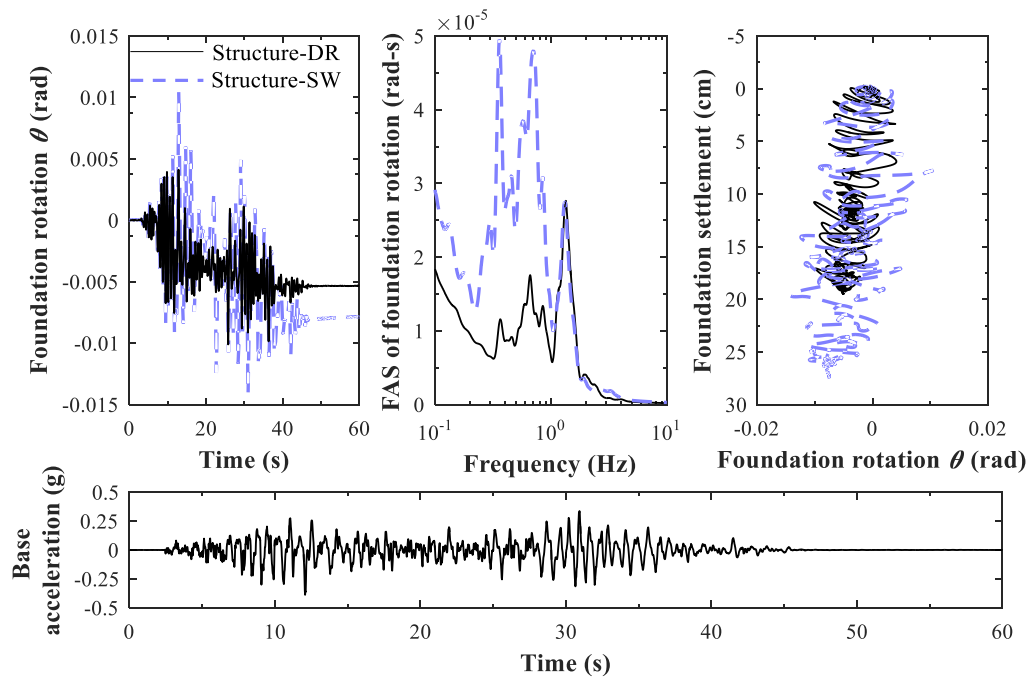
(b)

Fig. 4 – Foundation rotation (tilt) during: (a) Kobe; and (b) JoshuaT motions. Rotation towards the north is taken as positive.

These figures show that significant footing permanent rotation occurs in both structures during shaking. However, the residual (permanent) rotation for Structure-SW is minimal during the less intense, Kobe motion, suggesting that the structural wall mitigation effectively reduces the permanent tilt in Structure-SW compared to Structure-DR by limiting deviatoric strains. However, the restriction of excess pore pressure dissipation in the foundation soil underneath Structure-SW during the stronger, longer duration motion (JoshuaT) amplifies the magnitude of transient foundation rotation by 44% compared to Structure-DR. The permanent rotation of Structure-SW is also significant in the JoshuaT motion. The FAS of foundation rotation indicates a rocking fundamental frequency of approximately 0.4 Hz for both structures. Structure-SW experiences amplified low frequency content because the soil underneath is softened due to liquefaction. On the other hand, Structure-DR is not affected by liquefaction in the underlying soil, as it maintains low excess pore pressures under and adjacent to the building and the fundamental rocking frequency of Structure-DR follows that of the input motion more closely as a result.

4.3 Total, rocking, and flexural drift of the superstructure

The lateral displacement experienced by the building superstructure during a seismic event is associated with both rocking of the foundation (i.e., rigid-body rotation of the structure), and flexural deformation of structural elements. Often, this lateral displacement is represented through a dimensionless term called roof drift ratio, which is defined as the ratio of lateral displacement of the roof (with respect to the foundation) to the height of the structure. In this study we distinguish between rocking-induced lateral displacement, designated as rocking drift ratio (δ_R), and flexural deformation in columns, called flexural drift (δ_F). The sum of rocking and flexural drift gives the total drift ratio (δ_T). Fig. 5 details how the rocking, flexural, and total drift ratios are considered. The transient lateral displacements at the roof and base of the structure are estimated by double integrating horizontal accelerations at the roof. We focus on transient displacement because we did not expect permanent or inelastic drifts for the structural fuses used in this particular test. The vertical accelerometers at the foundation edges provide a measure of the rigid body rotation angle (θ). This angle can be substituted into Eq. (1) to estimate the transient rocking-induced lateral displacement at the roof of the structure, as described by Karimi and Dashti [22]. Prior to the integration, an acausal Butterworth band-pass filter with corner frequencies of 0.1 and 20 Hz was applied to acceleration time histories. Normalizing the total and rocking displacement by the height of the structure provides the corresponding drift ratio; the flexural drift ratio is the difference between the total and rocking drift ratios at a given time.

$$\delta_R = H\left[2(1-\cos\theta)\right]^{1/2} sign(\theta) \tag{1}$$
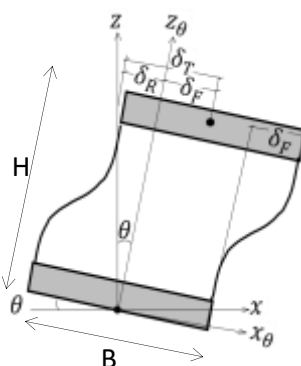

Fig. 5 – Drift definitions for a single-degree-of-freedom structure (Karimi and Dashti [22]).

Fig. 6 presents the time history and FAS of total, rocking, and flexural drift ratios of Structure-DR and Structure-SW during the Kobe and JoshuaT motions. The time history of total drift ratio during the Kobe motion suggests that Structure-SW experiences higher drifts than Structure-DR. As the larger excess pore pressures under Structure-SW soften the foundation soil, rocking-induced drifts are amplified. Overall, in terms of flexural

drift, both mitigation techniques perform well during the low intensity and short duration Kobe motion, and the structural responses are similar. Total drifts measured during the longer-duration JoshuaT are similar for Structure-DR and Structure-SW. Yet, Structure-DR experiences smaller transient foundation rotation by successfully dissipating excess pore pressures, which results in larger flexural drifts. Structure-SW, on the other hand, experiences larger foundation rotation during this motion because of soil liquefaction underneath, which results in a reduction of the flexural component of drift, and hence, a lower tendency for superstructure damage. In the Kobe motion, the FAS of the drift ratios indicate that amplification of drift happens at similar frequencies for both structures. However, in JoshuaT, Structure-SW sees a reduction in the higher frequency energy especially in the flexural drift spectra associated with liqexufaction.
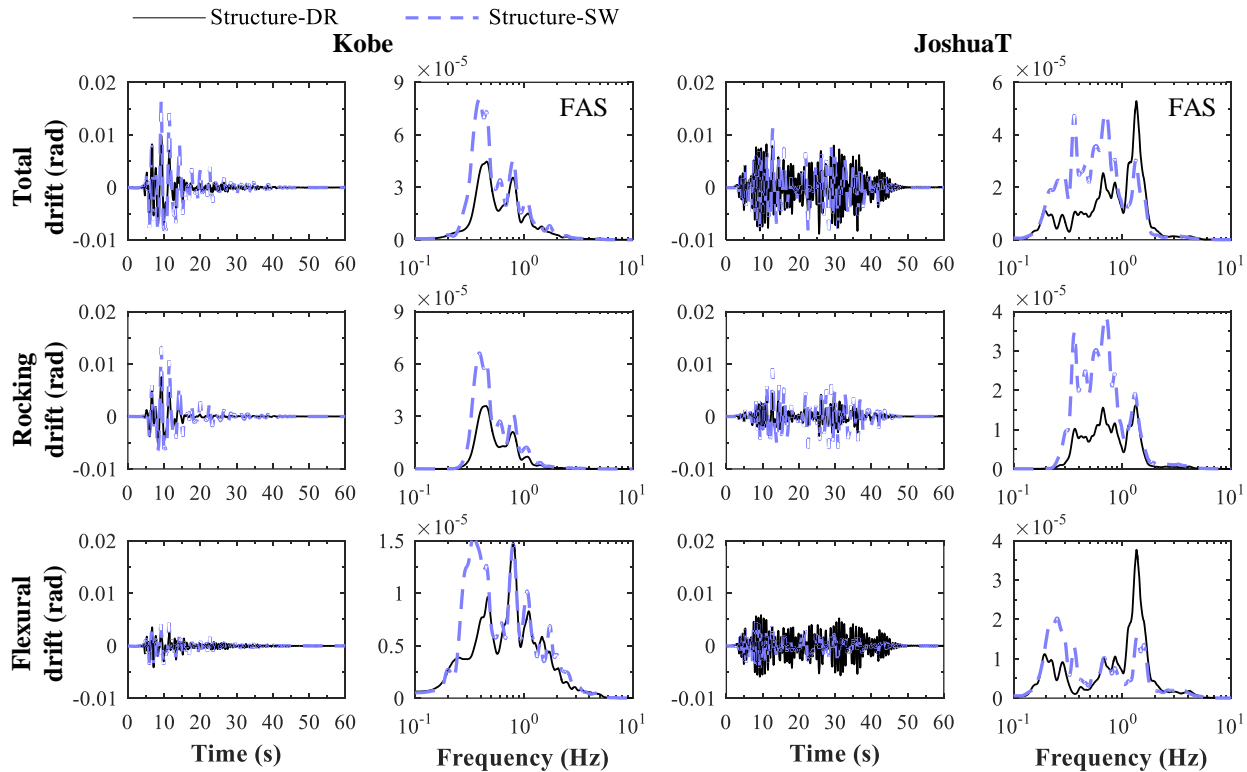

Fig. 6 – Total, rocking, and flexural drift ratios for Structures-DR and SW.

4.4 Moment rotation behavior of column fuses

The inelastic response of the structure is controlled by reducing the cross-sectional area of beams and columns near the connections, which are often called "fuses". These fuses are used to concentrate the inelastic deformation of frame at particular locations, and represent a "strong column weak beam" frame mechanism with hinging in beams and at the base of columns. Experimental results with the type fuses employed in this first experiment show that none of the ground motions are strong enough to yield the beam and column fuses. Hence, this paper focuses only on the elastic moment-transient flexural roof drift behavior of column fuses of both structures. Future studies will evaluate the influence of inelastic fuse behavior. The roof transient flexural drift gives the transient flexural deformation of the column, and the corresponding bending moment in the column fuse is measured using strain gauges.

Fig. 7 and

Fig. 8 show the moment-transient roof drift at column fuses for Structures-DR and SW, revealing that the maximum moment measured in Structure-DR and SW is almost same during the less intense Kobe motion. But the column moments are greater on Structure-DR by 22% during the stronger, longer-duration JoshuaT motion. Rapid drainage under Structure-DR during the JoshuaT motion likely causes the structure to deform more through flexure than rocking, and it leads to greater maximum bending moment demand in Structure-DR. For

Structure-SW, during the initial shaking period (time = 3 – 10 s) of the JoshuaT motion, the moment in the column fuse increases. However, when the excess pore pressure accumulation in the underlying soil approaches an R_u of 0.75 ~ 0.8, the flexural deformation in the structural element and the corresponding bending moment in column fuses of Structure-SW become negligible.

Fig. 8 compares the zoomed moment-roof drift behavior of the two column fuses during the JoshuaT motion at time t = 35 – 40s, where R_u reaches 0.9 under Structure-SW. These results show the strong influence of the timing and extent of excess pore pressure generation in soil on the moment demand imposed on the superstructure.
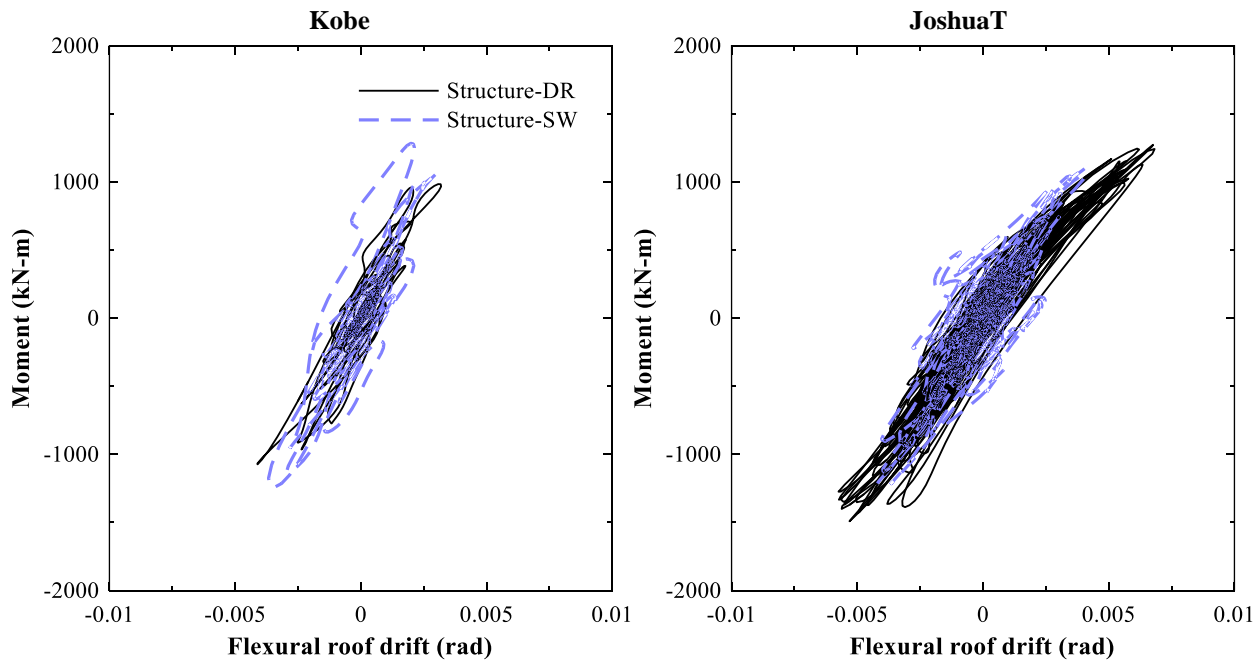
Fig. 7 – Moment-rotation behavior of column fuses of Structures-DR and SW during the Kobe and JoshuaT motions
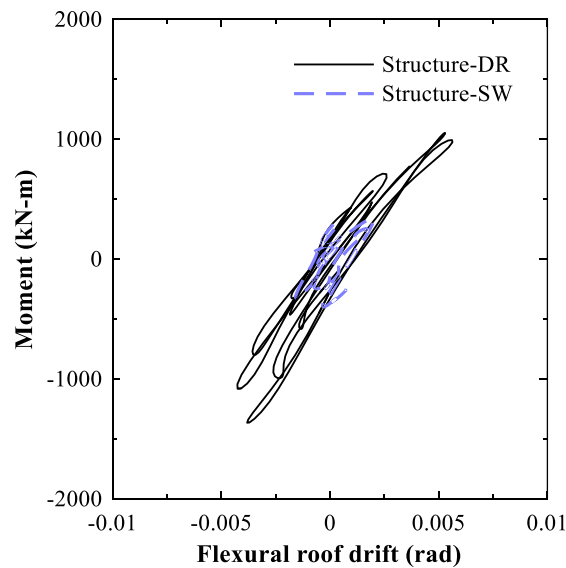

10

Fig. 8 – Moment-rotation of column fuses on Structures-DR and SW zoomed to time t = 35 − 40s during the JoshuaT motion.

5. Conclusions

In this study, the influence of liquefaction mitigation on soil and building response is studied through a centrifuge test. This test is one in a series of centrifuge experiments intended to evaluate the performance of a range of inelastic buildings on liquefiable ground with different mitigation techniques. The performance of the soil-foundation-structure-mitigation system on liquefiable ground strongly depends on the properties of the ground motion as well as the mechanisms of deformation that are active under a structure, which itself depends on the properties of the soil, structure, and mitigation strategy. Overall, enhanced drainage is shown to improve settlements and permanent tilt, but not flexural drift. A stiff structural wall is shown to limit deviatoric displacements and therefore, reduce total settlements, but only during weaker motions that do not generate liquefaction under the foundation. During stronger events, a structural wall can lead to liquefaction under the foundation by inhibiting flow, which can greatly increase the settlement and transient tilt of the foundation, but limit flexural drift and hence, damage to structural components.

6. Acknowledgements

7. Copyrights

8. References

[1] Liu L, Dobry R. (1997): Seismic response of shallow foundation on liquefiable sand. *Journal of Geotechnical and Geoenvironmental Engineering*, **123**(6), 557–567.

[2] Hausler EA (2002): Influence of ground improvement on settlement and liquefaction: A study based on field case history evidence and dynamic geotechnical centrifuge tests. *Ph.D. thesis*, University of California, Berkeley, USA.

[3] Dashti S, Bray J, Pestana J, Riemer M, Wilson D. (2010a): Centrifuge testing to evaluate and mitigate liquefaction-induced building settlement mechanisms. *Journal of Geotechnical and Geoenvironmental Engineering*, **136** (1), 151–164.

[4] Dashti S, Bray J, Pestana J, Riemer M, Wilson D. (2010b): Mechanisms of seismically induced settlement of buildings with shallow foundations on liquefiable soil. *Journal of Geotechnical and Geoenvironmental Engineering*, **136**(7), 918-929.

[5] Tokimatsu K, Seed HB. (1987): Evaluation of settlements in sands due to earthquake shaking. *Journal of Geotechnical Engineering*, **113** (8), 861– 878.

[6] Ishihara K, Yoshimine M. (1992): Evaluation of settlements in sand deposits following liquefaction during earthquakes. *Soils and Foundation*, **32**(1), 173–188.

[7] Stewart DP, Idriss IM, Boulanger RW, Hashash Y, Schmidt B. (1999): Mitigation of earthquake liquefaction hazards: a review of physical modeling studies. *Proceedings of 8th Australia-New Zealand Conference on Geomechanics*, Australia, **1**, 337–343.

[8] Balakrishnan A, Kutter BL. (1999): Settlement, sliding, and liquefaction remediation of layered soil. *Journal of Geotechnical and Geoenvironmental Engineering*, **125** (11), 968–978.

[9] Sasaki Y, Taniguchi E. (1982): Shake table test on gravel drain to prevent liquefaction of sand deposits. *Soils and Foundation*, **11** (3), 1-14.

[10] Kimura T, Takemura I, Hiro-oka A, OkaMura M, Matsuda T. (1995): Countermeasures against liquefaction of sand deposits with structures. *Proceedings of 1st International Conference Earthquake Geotechnical Engineering*. Tokyo, 163-184.

[11] Rollins KM, Anderson JKS, McCain AK, Goughnour RR. (2003): Vertical composite drains for mitigating liquefaction hazard. *Proceedings of 13th International Offshore and Polar Engineering Conference*, Hawaii, USA, 498-505.

[12] Howell R, Rathje EM, Kamai R, Boulanger R. (2012): Centrifuge modeling of prefabricated vertical drains for liquefaction remediation. *Journal of Geotechnical and Geoenvironmental Engineering*, **138**(3), 262-271.

[13] Tanaka H, Kita H, Iida T, Saimura Y. (1996): Countermeasure for liquefaction using steel sheet pile with drain capability. *Proceedings of International Conference on Engineering for Protection from Natural Disasters*, Bangkok, 643-655.

[14] Mason HB. (2011): Seismic performance assessment in dense urban environments. *Ph.D. thesis*, University of California, Berkeley, USA.

[15] Chen Z, Hutchinson TC, Trombetta NW, Mason HB, Bray JD, Jones KC, Bolisetti C, Whittaker AS, Choy BY, Fiegel GL, Montgomery J, Patel RJ, Reitherman RD. (2010): Seismic performance assessment in dense urban environments: evaluation of nonlinear building-foundation systems using centrifuge tests. *Proceedings of 5th International Conference on Recent Advances in Geotechnical Earthquake Engineering and Soil Dynamics*, Rolla, USA.

[16] Ko H-Y. (1988): The Colorado Centrifuge Facility. *Centrifuge 88*, 73–75.

[17] Ketchum SA. (1989): Development of an earthquake motion simulator for centrifuge testing and the dynamic response of a model sand embankment. *Ph.D. Thesis*, University of Colorado Boulder, USA.

[18] Ghayoomi M, Dashti S, McCartney JS. (2013): Performance of a transparent flexible shear beam container for geotechnical centrifuge modeling of dynamic problems. *Soil Dynamics and Earthquake Engineering*, **53**, 230–239.

[19] Stewart DP, Chen YR, Kutter BL. (1998): Experience with the use of methylcellulose as a viscous pore fluid in centrifuge models. *ASTM Geotechnical Testing Journal*, **21** (4), 365–369.

[20] Stringer ME, Madabhushi SPG. (2009): Novel computer-controlled saturation of dynamic centrifuge models using high viscosity fluids. *ASTM Geotechnical Testing Journal*, **23** (6), 1-6.

[21] Fiegel GL, Kutter BL. (1994): Liquefaction-induced lateral spreading of mildly sloping ground. *Journal of Geotechnical Engineering*, **120**(12), 2236–2243.

[22] Karimi Z, Dashti S. (2016): Seismic Performance of Structures on Liquefiable Soils: Insight from Numerical Simulations and Centrifuge Experiments. *Journal of Geotechnical and Geoenvironmental Engineering*, (In press).